

Agriculture and Forest Classification Using ISODATA Technique in Madikeri, Kodagu

G. A. ARPITHA, A. L. CHOODARATHNAKARA AND G. S. SINCHANA

Department of Electronics and Communication Engineering, Government Engineering College, Kushalnagar
Visvesvaraya Technological University, Belagavi - 590 018
e-Mail : arpithaga6@gmail.com

AUTHORS CONTRIBUTION

G. A. ARPITHA :
Framing the methodology,
data collection & analysis
and manuscript preparation;

A. L. CHOODARATHNAKARA :
Supervising and revising the
content;

G. S. SINCHANA :
Suggestions, editing and
revising the content of the
article

Corresponding Author :

G. A. ARPITHA

Received : August 2023

Accepted : March 2024

ABSTRACT

Remote sensing possesses a distinctive capability to survey extensive geographical areas of the Earth while gathering essential data pertinent to regions. LULC data play a crucial role in agricultural management and environmental conservation. The present study aims to map and monitor the Land Use Land Cover patterns of Madikeri Taluk, Kodagu District. The research employs the ISODATA clustering technique to automatically classify LULC patterns and analyze data from LANDSAT-8 satellite imagery captured in the year 2016. The findings of the analysis reveal PAN data alone achieved the Overall Classification Accuracy of 65.48 per cent, whereas the fused data, OCA increased to 66.47 per cent, resulting in difference of 0.99 per cent. The Kappa statistics obtained for the panchromatic and fused data is 0.572 and 0.5775 respectively. The agricultural land and forest regions identified for PAN data is 24.26 per cent and 24.57 per cent of the area. The agricultural land and forest regions identified using fused data is 10.37 and 28.29 per cent respectively. Hence, it is concluded that classification of forest and agricultural regions based on fused data yields superior results compared to that of panchromatic data.

Keywords : ISODATA, Kodagu, Landsat-8, Agriculture land, Forest region

REMOTE sensing is effective tool for determining land use land cover (LULC) estimation using appropriate datasets and classification approaches (Abdu, 2019). Land change science uses land LULC interchangeably, but with different meanings. Land usage refers to human activities on land. In contrast, Land Cover defines how much land is for farming, forest, aquatic, construction, etc (Dibs *et al.*, 2020). The study of LULC and its change is critical for understanding numerous environmental issues associated with urban and adjacent environments (Mishra and Palkar, 2015).

Unsupervised classification methods are extensively used in image identification and classification of LULC features. Numerous unsupervised classification

approaches are available in remote sensing (RS) and are widely used to categorize satellite images. Various unsupervised techniques have been employed by the researchers to accurately classify the features of land. ISODATA clustering method for the classification have been employed and the results demonstrated that the algorithm had efficient and speedy processing capabilities while dealing with remote sensing images (Li *et al.*, 2010). To create accurate LULC mapping for Baghdad the techniques such as Maximum Likelihood Classifier (MLC), Minimum Distance (MD) and Principal Component Analysis (PCA) are utilized. Landsat-8 imagery of 30 m resolution to conduct the analysis. The findings revealed that the MLC had an overall accuracy of 98.90 per cent compared to the other methods (Kaimaris *et al.*, 2020;

Zhang, 2004). Using the same satellite data and technique the study was conducted for Kashmir Valley from 1992 to 2015. Notable changes in LULC patterns were discovered with overall classification accuracy (OCA) of 91 per cent, producer's accuracy (PA) of 95 per cent and the user's accuracy (UA) of 95 per cent (Alam *et al.*, 2020).

In recent years, researchers improved the classification performance by utilizing several supervised machine-learning approaches. High-resolution worldview-3 imagery with a spatial resolution of 0.5 meters and four bands, including RGB and NIR was utilized for the classification using algorithms such as K-Nearest Neighbors (KNN), Xgboost, Random Forest (RF) and Support Vector Machine (SVM). Xgboost and SVM performed better yielding an accuracy of 80.1 per cent (Georganos *et al.*, 2018). The SVM technique is implemented in Upper Parana River Basin, South America for LULC classification. It has utilized Glob Cover land cover products, GlobeLand30, GLCNMO and MODIS sensor data with 300m, 30m, 500m resolution respectively. SVM achieved overall accuracy of 80 per cent. Hence, it is concluded that this technique offers better mapping of LC, exclusively for local studies (Mandal *et al.*, 2019). Landsat-8 OLI imagery is used in the study to estimate the usability of classifiers such as decision tree, naive Bayes, support vector machine and random trees in suburban area of Beijing, China. The overall accuracy of RT was 90 per cent (Rudke *et al.*, 2019). The Joint Deep Learning (JDL), CNN and MLP are the classification method was implemented using Landsat TM and Landsat ETM + with 30m resolution in Southampton and Manchester. The JDL obtained the OA of 90.18 per cent for LC and 87.92 per cent for LU. Authors have concluded that JDL technique works efficiently for identification of LULC for small-scale areas (Zhang *et al.*, 2019).

Spectral signatures of each class can be generated through unsupervised classification utilizing ISODATA clustering. ISODATA clustering algorithm has good adaptability and flexibility. This algorithm is extremely good at detecting spectral clusters in data.

This clustering employs a method in which all samples are assigned to present cluster centers throughout each iteration and new means are produced for each class. It classifies pixels into a predetermined number of unique spectral groups using spectral separation between pixels of an image in feature space (Sun *et al.*, 2017 and Li *et al.*, 2010). Therefore, ISODATA clustering technique is employed in present study.

The primary goal of this research is to examine ISODATA classifiers for extracting agriculture and forest features in Madikeri Taluk, Kodagu District. The investigation utilized the LANDSAT-8 satellite imagery and relied on the Erdas Imagine 9.2 software platform as the primary tool for data analysis. The article is structured as follows: The first section consists introduction, overview of LULC classification techniques. Second sections detail the study area and proposed methodology. The third section presents the analysis of the obtained results. Final section summarizes the essential findings and draws conclusions based on the outcomes of the study.

MATERIAL AND METHODS

Study Area

Madikeri region is characterized by a tropical climate owing to its elevation of 1,150 meters and geographically situated at 12.42°N 75.73°E, renowned for its coffee plantations and vibrant tourism industry (Dikpal, 2022 and Putty *et al.*, 2021). As shown in Fig. 1, Madikeri is positioned within the Western Ghats and is widely recognized as a popular hill station (Setiyawan, 2017 and Ashrit *et al.*, 2020). As shown in Table 1, Landsat-8 data is obtained from the United States Geological Survey and utilized in the analysis.

TABLE 1

Satellite data product used for analysis

Satellite and data type	Date of acquisition	Spatial Resolution
LANDSAT-8	27 March 2016	15m

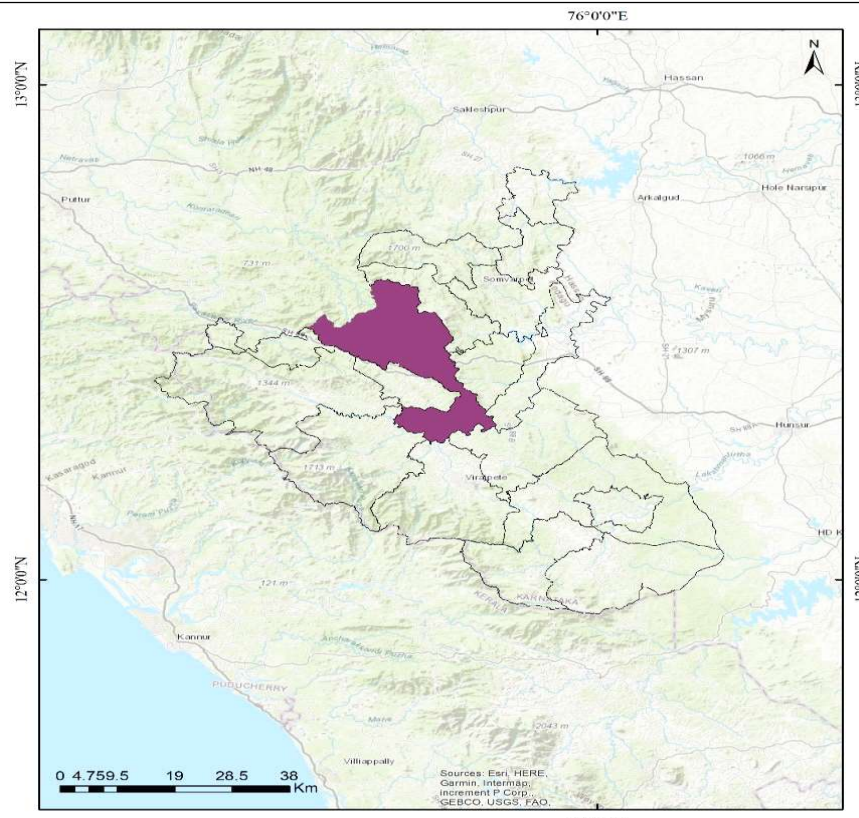


Fig. 1 : Madikeri, Kodagu

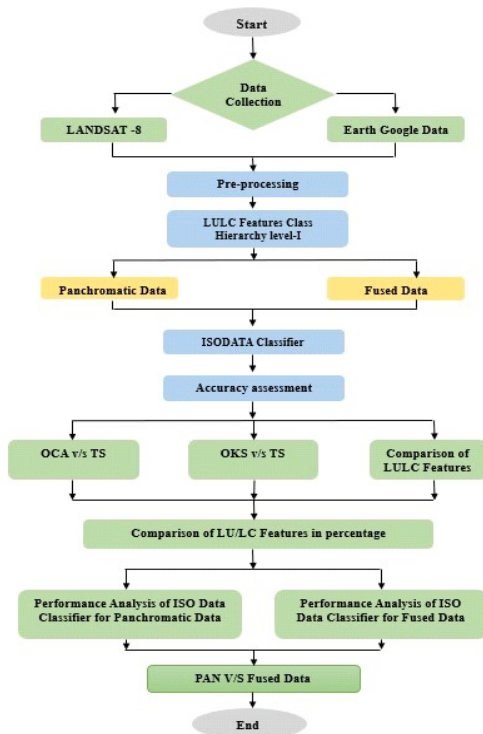


Fig. 2 : Methodology for extraction of LULC features using unsupervised ISODATA

Pre-Processing of Satellite Imagery

LANDSAT-8 satellite image data collected from U.S. Geological Survey (USGS) in the year 2016. Pre-processing of the satellite image was carried out in employed by ERDAS Imagine 9.2. The preprocessing is performed in the following manner as shown in Fig. 2.

Geo-correction : Geo-correction aim to eliminate positional inaccuracies and recreate the original image with the geometrical features of a map.

Sub-setting : The satellite image will have wider coverage than the necessary study area. Consequently, a smaller area known as a subset must be created from the broader image.

Fusion of image : Fusion uses an algorithm to combine two or more layers to extract better details about an LULC features of the study area.

Accuracy Assessment

a. The Error Matrix

An N*N error matrix is used to evaluate the classification model. The numbers in the columns indicate ground truth, while the numbers in the rows represent the categorization outcome. This square matrix contains pixels correctly categorized along the major diagonal. The overall user accuracy and producer accuracy are calculated using the error matrix.

b. Overall Accuracy

Overall accuracy represents the correctly classified pixels. The error matrix presented in equation (1) can be used to determine the overall accuracy of the system.

$$OA = \frac{\sum_{K=1}^N a_{kk}}{\sum_{i,k=1}^N a_{ik}} = \frac{1}{n} \sum_{K=1}^N a_{kk} \quad \dots(1)$$

c. Kappa Statistics

The Kappa statistic is based on the difference between the actual agreement in the error matrix

and the chance agreement, which is represented by the row and column total.

RESULTS AND DISCUSSION

ISODATA Classification of Panchromatic Image

The panchromatic band of Landsat-8 of 15 m spatial resolution is used in this study. The panchromatic data combines variety of wavelengths and bands, such as the thermal infrared or visible. Fig. 3. depicts the result of the Panchromatic ISODATA classified data. Table 2 represents the confusion matrix and corresponding kappa values derived by ISODATA technique to classify seven classes using different validation point quantities such as 36, 67, 100, 135 and 168. The OCA for 36 validation points was recorded as 50 per cent, while for 67, 100, 135 and 168 validation points, the accuracies obtained was 53.73 per cent, 57 per cent, 61.48 per cent and 65.48 per cent, respectively. The Kappa Statistics, exhibits 0.0588 for 36 validation points, 0.2654 for 67 validation points, 0.3474 for 100 validation points, 0.4837 for 135 validation points and 0.3783 for 168 validation points.

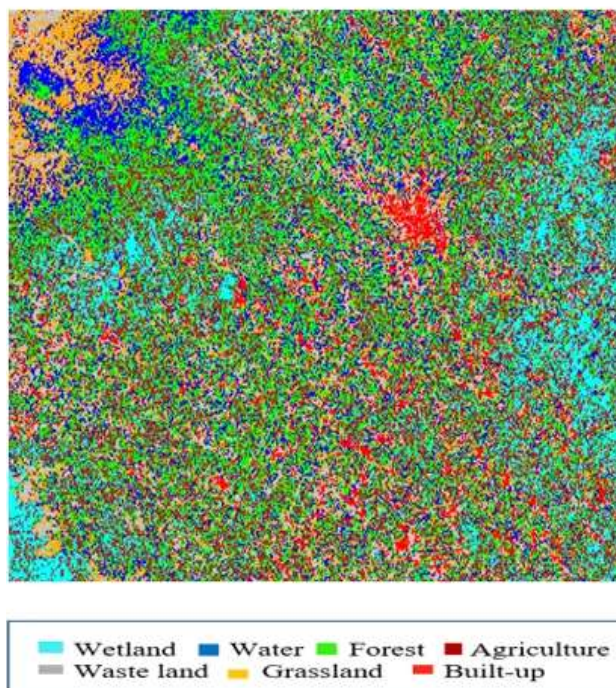


Fig. 3 : ISODATA classified LANDSAT-8 PAN Image

TABLE 2
Confusion Matrix for ISODATA classified Panchromatic Image with different values

Classes	1	2	3	4	5	6	7	RT	UA in %	Kappa
Confusion Matrix for ISODATA Classified Panchromatic Image with VS=36										
1	1	7	0	0	0	1	0	9	11.11	0.0588
2	0	10	0	0	0	0	0	10	100	1.0000
3	0	1	1	0	1	0	0	3	33.33	0.2941
4	0	3	0	1	0	1	0	5	20	0.1771
5	1	0	1	0	1	0	0	3	33.33	0.2727
6	0	1	0	0	1	2	0	4	50	0.4375
7	0	0	0	0	0	0	2	2	100	1.0000
CT	2	22	2	1	3	4	2	36		
PA in%	50	45	50	100	33.33	50	100			
Confusion Matrix for ISODATA Classified Panchromatic Image with VS=67										
1	6	0	10	0	0	0	0	16	37.50	0.2654
2	1	3	4	0	0	0	0	8	37.50	0.3353
3	0	0	16	0	0	0	0	16	100	1.0000
4	0	1	5	3	0	1	0	10	30	0.2556
5	2	0	0	0	2	1	0	6	33.33	0.3128
6	0	0	2	1	0	3	0	7	42	0.3825
7	1	0	0	0	0	0	3	4	75	0.7298
CT	10	4	37	4	2	5	5	67		
PA in%	60	75	43	75	100	60	60			
Confusion Matrix for ISODATA Classified Panchromatic Image with VS=100										
1	11	12	1	0	0	0	0	24	45	0.3474
2	0	25	0	0	0	0	1	26	96	0.9167
3	3	0	5	1	0	0	1	10	50	0.4505
4	1	6	1	7	0	0	0	15	46	0.4203
5	0	6	0	0	3	1	0	10	30	0.2784
6	1	4	1	0	0	4	1	11	36	0.3301
7	1	0	1	0	0	0	3	5	60	0.5745
CT	17	52	9	8	3	5	6	100		
PA in%	64.70	48.07	55.55	87.5	100	80	50			
Confusion Matrix for ISODATA Classified Panchromatic Image with VS=135										
1	20	12	0	0	0	1	0	33	60.61	0.4837
2	1	32	0	0	0	0	0	33	96.97	0.9432
3	5	1	6	0	0	0	1	13	46.15	0.4276
4	1	9	0	8	0	0	2	20	40	0.3622
5	1	8	1	0	4	0	0	14	28.57	0.2639
6	2	1	1	0	0	8	3	15	53.33	0.50000

Continued....

TABLE 2 Continued....

Classes	1	2	3	4	5	6	7	RT	UA in %	Kappa
7	2	0	0	0	0	0	5	7	71.43	0.6889
CT	32	63	8	8	4	9	11	135		
PA in%	62.50	50.79	75	100	100	88.89	45.45			

Confusion Matrix for ISODATA Classified Panchromatic Image with VS=168

1	19	20	0	0	0	1	1	41	46.34	0.3783
2	0	41	0	0	0	0	0	41	100	1.000
3	3	1	10	0	1	0	1	16	62.50	0.5962
4	1	7	1	13	0	0	3	25	52	0.4797
5	0	11	0	0	6	0	0	17	35.29	0.3248
6	0	5	1	0	0	13	0	19	68.42	0.6555
7	0	1	0	0	0	0	8	9	88.50	0.8796
CT	23	86	14	13	7	14	13	168		
PA in%	82.61	47.67	71.42	100	85.71	92.86	61.54			

Legend : 1 = Agriculture, 2 = Forest, 3 = Waste lands, 4 = Water bodies, 5 = Wet lands, 6 = Grass land, 7 = Built up, RT = Row Total, CT = Column Total

ISODATA Classification of Fused Image

This study obtained a fused image by combining LANDSAT-8 bands such as PAN, 2, 3 and 5 as illustrated in Fig. 4. Table 3 presents the confusion matrix and corresponding kappa values for the ISODATA Technique applied to classify seven classes using different validation point quantities: 35, 65, 100, 135 and 167. The analysis revealed that with 35 validation points, the overall classification accuracy was 51.43 per cent. When the validation points were increased to 65, 100, 135 and 167, the overall accuracy improved to 55.38 per cent, 58.43 per cent, 62.96 per cent and 66.47 per cent, respectively. The Kappa Statistics, which provide a measure of agreement beyond chance, were found to be 0.1532 for 35 validation points, 0.3705 for 65 validation points, 0.5914 for 100 validation points, 0.5844 for 135 validation points and 0.5990 for 167 validation points.

Performance Analysis of Panchromatic Image and Fused Image for ISODATA

The ISODATA algorithm was applied to both panchromatic and fused images obtained from

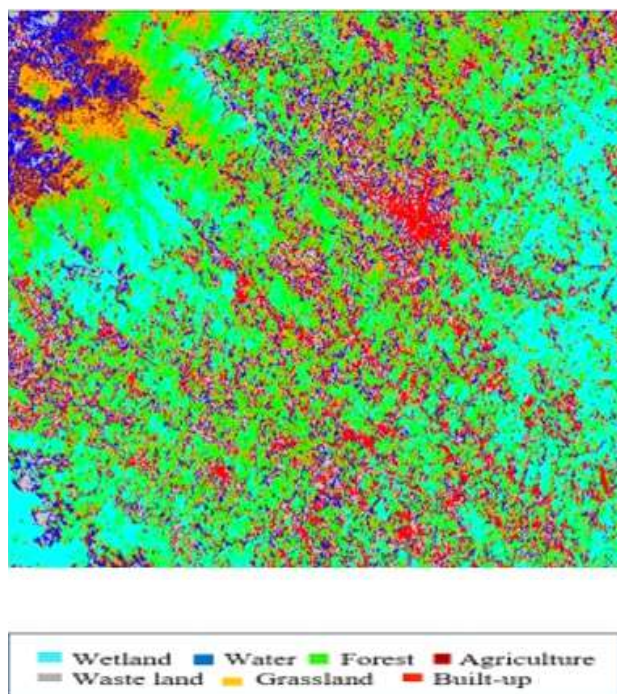


Fig. 4 : ISODATA classified LANDSAT-8 Fused Image

LANDSAT-8. The Landsat panchromatic band consisted of a 15-meter pixel resolution (Fig. 5) illustrates the OCA versus the training samples for the PAN and fused images processed through the

TABLE 3
Confusion Matrix for ISODATA classified Fused Image with different values

Classes	1	2	3	4	5	6	7	RT	UA in %	Kappa
Confusion Matrix for ISODATA Classified Fused Image with VS=35										
1	1	2	0	0	0	1	0	4	25	0.1532
2	0	8	0	0	2	0	0	10	80	0.5882
3	1	0	2	0	0	0	0	3	66.67	0.6465
4	1	1	0	1	0	0	0	3	33.33	0.3137
5	0	5	0	0	2	0	0	7	28.57	0.1667
6	0	2	0	0	1	3	0	6	50	0.4355
7	1	0	0	0	0	0	1	2	50	0.5853
CT	4	18	2	1	5	4	1	35		
PA in%	25	44.44	100	100	40	75	100			
Confusion Matrix for ISODATA Classified Fused Image with VS=65										
1	3	2	1	0	0	0	1	7	42	0.3705
2	0	17	0	0	1	0	0	18	94.44	0.8663
3	1	2	2	0	0	1	0	6	33.33	0.3011
4	1	3	0	2	0	0	0	6	33.33	0.3132
5	0	9	0	0	5	0	0	14	35.71	0.2796
6	0	5	0	0	1	5	0	11	45.45	0.3991
7	1	0	0	0	0	0	2	3	66.67	0.6505
CT	6	38	3	2	7	6	3	65		
PA in%	50	44.44	66.67	100	71.43	83.33	66.67			
Confusion Matrix for ISODATA Classified Fused Image with VS=100										
1	7	3	1	0	0	0	0	11	63.64	0.5914
2	0	27	1	0	0	0	0	28	96.43	0.9224
3	1	0	5	0	1	2	0	9	55.56	0.5116
4	1	4	1	2	0	1	0	9	22.22	0.1898
5	0	11	0	1	9	0	0	21	42.86	0.6379
6	1	9	1	1	0	5	0	17	29.41	0.2327
7	1	0	0	0	1	0	3	5	60	0.5876
CT	11	54	9	4	11	8	3	100		
PA in%	63.644	50	55.56	50	81.82	62.50	100			
Confusion Matrix for ISODATA Classified Fused Image with VS=135										
1	9	3	2	0	0	0	0	14	64.29	0.5844
2	0	38	0	0	0	0	0	38	100	1.0000
3	6	2	5	0	0	0	0	13	38.46	0.3407
4	1	1	2	6	0	2	0	12	50	0.4767
5	0	17	0	0	12	0	0	29	41.38	0.3566
6	1	11	0	0	0	10	0	22	45.45	0.4013

Continued....

TABLE 3 Continued....

Classes	1	2	3	4	5	6	7	RT	UA in %	Kappa
7	2	0	0	0	0	0	5	7	71.43	0.7033
CT	19	72	9	6	12	12	5	135		
PA in%	47.39	52.78	55.5	100	100	83.33	100			

Confusion Matrix for ISODATA Classified Fused Image with VS=167

1	11	4	2	0	0	0	0	17	64.71	0.5990
2	1	45	0	0	0	1	0	47	95.74	0.9154
3	2	4	8	0	0	0	2	16	50	0.4542
4	2	5	1	7	0	0	0	15	46.67	0.4433
5	0	16	3	0	16	0	0	35	45.71	0.3996
6	0	9	0	0	0	19	0	28	67.86	0.6348
7	4	0	0	0	0	0	5	9	55.56	0.5361
CT	20	83	14	7	16	20	7	167		
PA in%	55	54.14	57.14	100	100	95	71.43			

Legend : 1 = Agriculture, 2 = Forest, 3 = Waste lands, 4 = Water bodies, 5 = Wet lands, 6 = Grass land, 7 = Built up, RT = Row Total, CT = Column Total

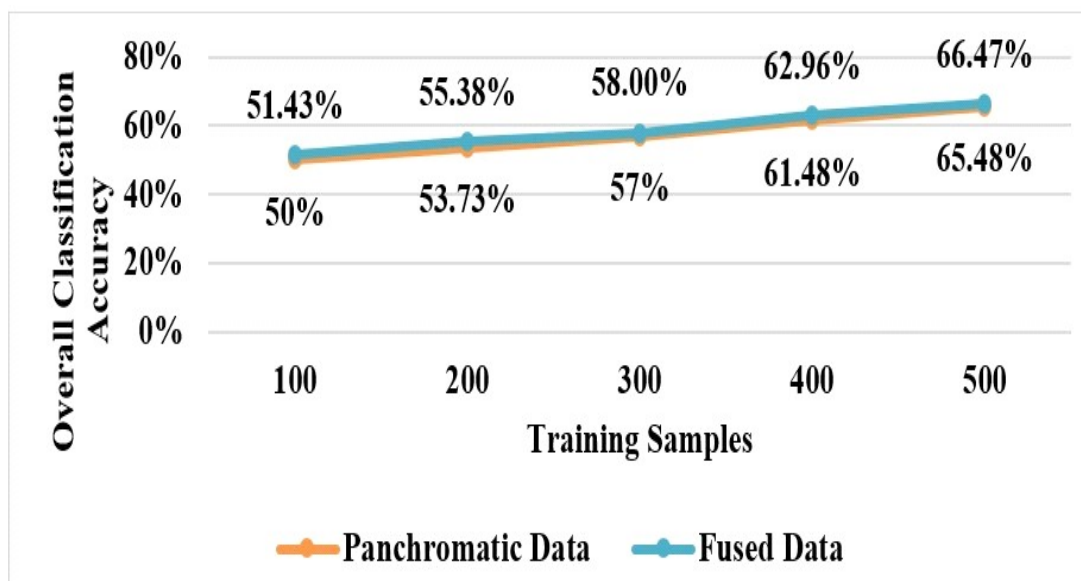


Fig. 5 : Comparison of OCA v/s Training Sample PAN Image and Fused image for ISODATA

ISODATA algorithm. The results indicated that the panchromatic data achieved an OCA of 50 per cent, while the fused data exhibited 51.43 per cent for the 100-training set. With an increase in the number of training sets 200, 300, 400 and 500, the accuracy improved to 53.75 per cent, 57 per cent, 61.48

per cent and 65.48 per cent for panchromatic data and 55.38 per cent, 58 per cent, 62.96 per cent and 66.47 per cent for fused data.

Fig. 6 compares the OKS versus the training samples for both PAN and fused images when subjected to the

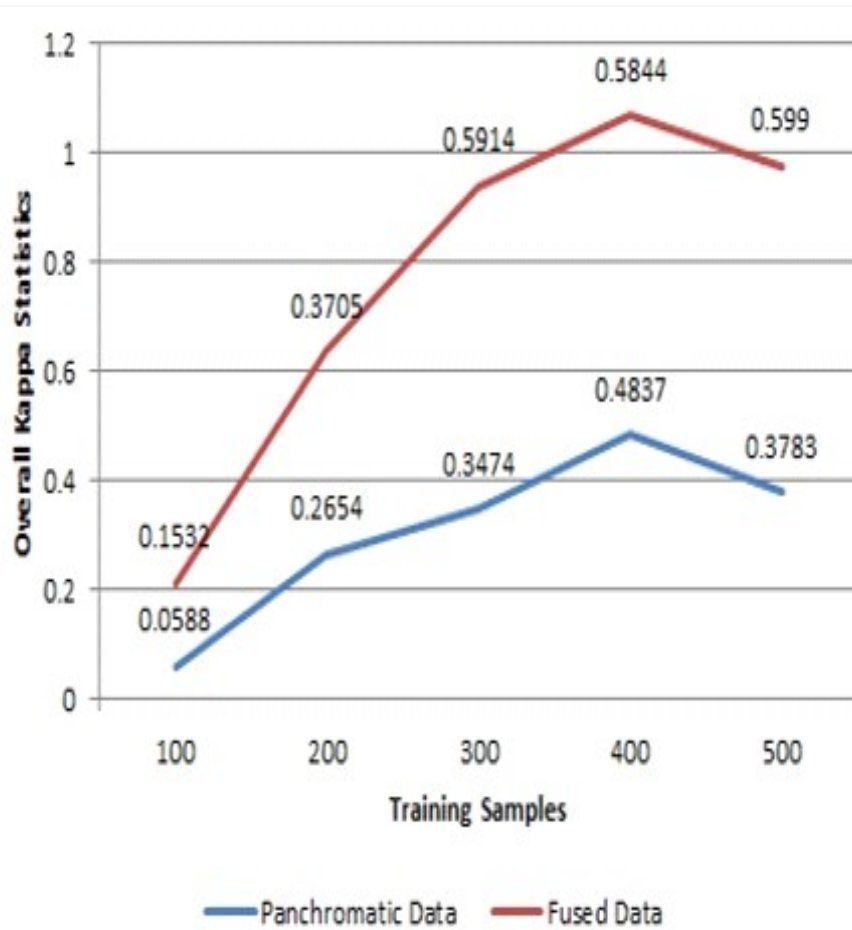


Fig. 6 : Comparison of OKS v/s Training Sample PAN Image and Fused image for ISODATA

ISODATA algorithm. For the 100-training set, the panchromatic data yielded an OKS of 0.0588, while the fused data exhibited an OKS of 0.1532. More over, for the 200, 300, 400 and 500 training sets, the panchromatic data achieved OKS values of 0.2654, 0.3474, 0.4837 and 0.3783, respectively, whereas the fused data achieved OKS values of 0.3705, 0.5914, 0.5844 and 0.5990, respectively.

The Table 4 and 5 provides a breakdown of the classifications observed in the Madikeri region and presents an overview of LULC features, considering multiple parameters such as pixel count, acreage, hectare measurement and percentage area. The Table 4 encompasses the classification of the entire study area, which spans 4,930.644 hectares. Notably,

TABLE 4
ISODATA Classification of LANDSAT -8 PAN data

Classes	Area in pixels	Area in Acres	Area in Hectares	Area in %
Unclassified	9292	34.442	13.938	0.28%
Wetland	326959	1211.900	490.4385	9.95%
Water	483447	1791.936	725.1705	14.71%
Forest	807666	2993.680	1211.499	24.57%
Agriculture	797558	2956.213	1196.337	24.26%
Waste land	320785	1189.016	481.1775	9.76%
Grass land	363708	1348.113	545.562	11.06%
Built up	177681	658.589	266.5215	5.41%
Total	3287096	12183.888	4930.644	100.00%

TABLE 5
ISODATA Classification of LANDSAT - 8
Fused image

Classes	Area in pixels	Area in Acres	Area in Hectares	Area in %
Unclassified	8816	65.35	26.448	0.27%
Wetland	691339	5125.01	2074.017	21.04%
Water	296511	2198.08	889.533	9.03%
Forest	929296	6889.02	2787.888	28.29%
Agriculture	340734	2525.92	1022.202	10.37%
Waste land	302398	2241.73	907.194	9.21%
Grass land	542698	4023.11	1628.094	16.52%
Built up	173296	1284.67	519.888	5.28%
Total	3285088	24352.89	9855.264	100.00%

within the Madikeri region, the forest class has been identified as the most prominently classified category, covering an area of 24.57 per cent. Conversely, the built-up class has received the lowest classification, representing an area of 5.41 per cent compared to the other classes in the region. Table 5 presents the classification of LULC features within 9,855.264 hectares. Among the various classes, the forest class has been identified as the most extensively classified,

covering an area of 28.29 per cent. On the other hand, the built-up class exhibits the lowest classification, representing only 5.28 per cent of the total area compared to the other classes in the region.

Fig. 7. compares LULC features between the PAN and Fused data processed through the ISODATA algorithm. The graph reveals valuable insights regarding the relative areas of different LULC classes. It is observed that the unclassified land class occupies the smallest area, accounting for 0.28 per cent of the panchromatic data and 0.27 per cent in the fused image. Conversely, the forest class exhibits the most significant area, with the panchromatic image showing coverage of 24.57 per cent and the fused image demonstrating a higher proportion of 28.29 per cent.

This research utilizes LANDSAT 8 satellite data to apply ISODATA classifiers to classify agricultural and forest land. The assessment of the technique reveals an accuracy of 65.48 per cent for panchromatic data and 66.47 per cent for fused data. Moreover, the ISODATA technique yields an Overall Kappa Statistic (OKS) of 0.3783 for panchromatic data and 0.5990 for fused data. It is observed that the agricultural land identified using panchromatic data

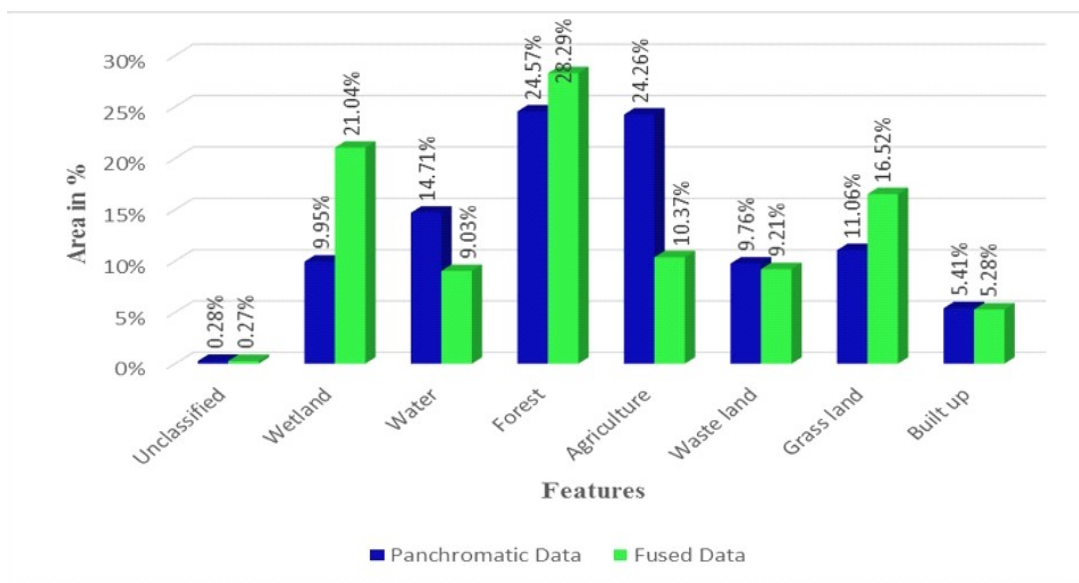


Fig. 7 : Comparison of LULC features of PAN Image and Fused image for ISODATA

encompasses 24.26 per cent of the study area. The fused data indicates a lower proportion of agricultural land at 10.37 per cent. In contrast, the forested areas identified using panchromatic data cover 24.57 per cent of the area, whereas the fused data suggest a higher percentage of forested areas at 28.29 per cent. Consequently, based on these findings, fused data outperforms the PAN data in accurately classifying agricultural land using ISODATA techniques.

Acknowledgments : We express our sincere gratitude to the following students for their invaluable assistance in experimenting: Rashmi Raju Gowda (USN: 4GL17EC031), Sowndarya. R. M (USN: 4GL17EC040), Varsha M (USN: 4GL17EC044) and Nishchitha, H. B. (USN: 4GL18EC411) from the Department of Electronics and Communication Engineering, GEC, Kushalnagara. Their contributions were greatly appreciated and played a crucial role in the successful execution of the experiment.

REFERENCES

- ABDU, H. A., 2019, Classification accuracy and trend assessments of land cover-land use changes from principal components of land satellite images. *International Journal of Remote Sensing*, **40** (4) : 1275 - 1300. <https://doi.org/10.1080/01431161.2018.1524587>.
- ALAM, A., BHAT, M. S. AND MAHEEN, M., 2020, Using landsat satellite data for assessing the land use and land cover change in Kashmir valley. *Geo Journal*, **85** (6) : 1529 - 1543. <https://doi.org/10.1007/s10708-019-10037-x>.
- ASHRIT, R., SHARMA, K., KUMAR, S., DUBE, A., KARUNASAGAR, S., ARULALAN, T., MAMGAIN, A., CHAKRABORTY, P., KUMAR, S., LODH, A., DUTTA, D., MOMIN, I., BUSHAIR, M. T., PRAKASH, B. J., JAYAKUMAR, A. AND RAJAGOPAL, E. N., 2020, Prediction of the august 2018, heavy rainfall events over Kerala with high resolution NWP models. *Meteorological Applications*, **27** (2) : 1 - 14. <https://doi.org/10.1002/met.1906>.
- DIBS, H., HASAB, H. A., AL-RIFAIE, J. K. AND AL-ANSARI, N., 2020, An optimal approach for land-use / land-cover mapping by integration and fusion of multispectral landsat OLI images: case study in Baghdad, Iraq. *Water, Air and Soil Pollution*, **231** (9). <https://doi.org/10.1007/s11270-020-04846-x>.
- GEORGANOS, S., GRIPPA, T., VANHUYSSSE, S., LENNERT, M., SHIMONI, M., KALOGIROU, S. AND WOLFF, E., 2018, Less is more: Optimizing classification performance through feature selection in a very-high-resolution remote sensing object-based urban application. *GIScience and Remote Sensing*, **55** (2) : 221 - 242. <https://doi.org/10.1080/15481603.2017.1408892>.
- KAIMARIS, D., PATIAS, P., MALLINIS, G. AND GEORGIADIS, C., 2020, Data fusion of scanned black and white aerial photographs with multispectral satellite images. *Sci.*, **2** (2). <https://doi.org/10.3390/sci2020029>
- DIKPAL, L. D. R., 2022, Landslide susceptible zonation mapping of Madikeri taluk, Kodagu district of Karnataka, India using Remote Sensing and Geographic Information System Techniques. *Interantional Journal of Scientific Research in Engineering and Management*, **6** (01). <https://doi.org/10.55041/ijrem11464>.
- LI, B., ZHAO, H. AND LV, Z. H., 2010, Parallel ISODATA clustering of remote sensing images based on MapReduce. Proceedings - 2010 International Conference on Cyber-Enabled Distributed Computing and Knowledge Discovery, CyberC **2010** : 380 - 383. <https://doi.org/10.1109/CyberC.2010.75>.
- MANDAL, J., GHOSH, N. AND MUKHOPADHYAY, A., 2019, Urban growth dynamics and changing land-use land-cover of megacity Kolkata and its environs. *Journal of the Indian Society of Remote Sensing*, **47** (10) : 1707 - 1725. <https://doi.org/10.1007/s12524-019-01020-7>.
- MISHRA, D. AND PALKAR, B., 2015, Image fusion Techniques: A review. *International Journal of Computer Applications*, **130** (9) : 7 - 13. <https://doi.org/10.5120/ijca2015907084>.
- PUTTY, M. R. Y., PRITHVIRAJ, B. N., KUMAR, P. N., NITHISH, M. G., GIRI, G. AND CHANDRAMOULI, P. N., 2021,

An insight into the hydrological aspects of landslides of 2018 in Kodagu, South India. *Landslides*, **18** (5) ; 1597 - 1610. <https://doi.org/10.1007/s10346-020-01589-y>.

RUDKE, A. P., FUJITA, T., ALMEIDA, D. S. DE, EIRAS, M. M., XAVIER, A. C. F., RAFEE, S. A. A., SANTOS, E. B., MORAIS, M. V. B. DE, MARTINS, L. D., SOUZA, R. V. A. DE, SOUZA, R. A. F., HALLAK, R., FREITAS, E. D. DE, UVO, C. B. AND MARTINS, J. A., 2019, Land cover data of upper Parana River Basin, South America at high spatial resolution. *International Journal of Applied Earth Observation and Geoinformation*, **83** (February), 101926. <https://doi.org/10.1016/j.jag.2019.101926>.

SETIYAWAN, Y., 2017, *Gadgil Report on the Western Ghats*. pp. : 1 - 14.

SUN, W., TIAN, Y., MU, X., ZHAI, J., GAO, P. AND ZHAO, G., 2017, Loess landslide inventory map based on GF-1 satellite imagery. *Remote Sensing*, **9** (4) : 1 - 17. <https://doi.org/10.3390/rs9040314>.

ZHANG, C., SARGENT, I., PAN, X., LI, H., GARDINER, A., HARE, J. AND ATKINSON, P. M., 2019. Joint deep learning for land cover and land use classification. *Remote Sensing of Environment*, **221** (May 2018) : 173 - 187. <https://doi.org/10.1016/j.rse.2018.11.014>.

ZHANG, Y., 2004, Understanding image fusion. *Photogrammetric Engineering and Remote Sensing*, **70** (6) : 657 - 661.